MCB
Journals.ASM.org

Defying DNA Double-Strand Break-Induced Death during Prophase I Meiosis by Temporal TAp63α Phosphorylation Regulation in Developing Mouse Oocytes

Dal-Ah Kim,[a] Eun-Kyung Suh[a,b]

Division of Life and Pharmaceutical Sciences[a] and Department of Life Sciences, College of Natural Sciences,[b] Ewha Womans University, Seoul, South Korea

The dichotomy in DNA damage sensitivity of developing mouse oocytes during female germ line development is striking. Embryonic oocytes withstand hundreds of programmed DNA double-strand breaks (DSBs) required for meiotic recombination. Postnatal immature oocytes fail to tolerate even a few DSBs induced by gamma radiation treatment. TAp63α, a p53 family member, undergoes phosphorylation and mediates postnatal immature oocyte death following gamma radiation treatment, which is thought important for germ line quality maintenance. Whether prenatal meiotic oocytes tolerate DNA DSBs simply because they lack TAp63α expression is not clear. We found a significant number of oocytes in newborn mice initiate TAp63α expression and simultaneously carry meiotic DNA DSBs. However, the risk of premature death appears unlikely, because newborn oocytes strongly abate TAp63α phosphorylation induction and resist normally lethal doses of ionizing radiation damage. A calyculin A-sensitive Ser/Thr phosphatase activity downregulates TAp63α phosphorylation and ATM kinase mediates phosphorylation. Possible alterations in the relative balance of these counteracting activities during development may first temper TAp63α phosphorylation and death induction during meiotic DNA DSB repair and recombination, and afterward, implement germ line quality control in later stages. Insights into inherent DNA DSB resistance mechanisms in newborn oocytes may help prevent infertility in women in need of radiation or chemotherapy.

Long-term maintenance of female fertility depends on the proper balance of life and death decisions in oocytes during development. In humans, approximately 7 million oocytes are made during embryogenesis, and this number diminishes to 1 to 2 million by birth, which is a massive loss of >85% (1). Significant loss of oocytes also occurs in mice, from ~25,000 at embryonic day 13.5 (E13.5) (2) to ~10,000 by birth (3, 4). Over the course of pre- and postnatal development, >99.9% of total oocytes undergo death (1). Nevertheless, a sufficient number somehow survive into adulthood and provide for female fertility (5, 6). The mechanisms that select oocytes for death or survival during development in mammals are not well understood (1, 6).

TAp63α, one of multiple p63 isoforms and a member of the p53 tumor suppressor family of transcription factors (7–10) is required for oocyte death in postnatal ovaries upon ionizing radiation (IR)-induced DNA damage. Postnatal immature primordial follicle oocytes in meiosis I arrest, or dictyate arrest, express TAp63α at high levels (11–13). Upon low-dose IR treatment of just 0.3 Gy, TAp63α is activated by phosphorylation and all immature primordial follicle oocytes undergo death and loss within a single day (11). Thus, immature primordial follicle oocytes are extremely DNA damage-sensitive cells. Interestingly, dictyate oocytes in secondary or larger follicles undergoing growth and maturation survive IR treatment (11), perhaps owing to downregulated TAp63α expression. The mechanism of IR-induced immature primordial follicle oocyte death appears to involve TAp63α phosphorylation-mediated TAp63α protein tetramerization and transcriptional activation of the downstream proapoptotic target genes for NOXA and PUMA (14–16). By eliminating DNA-damaged oocytes following low-level DNA damage, TAp63α function is thought to be important for maintaining the quality of the female germ line (12, 13). However, such high-stringency culling of the germ line could also result in rapid depletion of oocytes and accelerate the onset of infertility (17), since oocytes are largely made before birth and generally believed to be irreplaceable if lost during postnatal life (18). TAp63α activation can be inhibited by using a chemical inhibitor of the c-Abl kinase, imatinib, to reduce cisplatin-induced oocyte death (17). However, recent studies have challenged this finding (13, 19, 20), suggesting the advent of other approaches necessary for clinical use to protect DNA damage-sensitive oocytes during chemo- or radiation therapy. Whether oocytes have endogenous mechanisms to modulate TAp63α activity has not yet been considered.

Unlike postnatal dictyate stage oocytes, younger prenatal oocytes undergoing meiotic recombination withstand astonishingly several hundred meiotic DNA double-strand breaks (DSBs). DNA DSBs initiate homologous recombination and homologous chromosome exchange, which are important for genetic diversification of gametes. Spo11 induces meiotic DNA DSBs in the leptotene stage of prophase I meiosis around E14 in females (21, 22). Starting from around the E15 and E16 stages, homologous chromosomes harboring DSBs pair and synapse during the zygotene and pachytene stages of prophase I and undergo recombination (22). Recombined homologous chromosomes desynapse in the

Received 23 September 2013 **Returned for modification** 22 October 2013
Accepted 28 January 2014
Published ahead of print 10 February 2014
Address correspondence to Eun-Kyung Suh, esuh@ewha.ac.kr.
Supplemental material for this article may be found at http://dx.doi.org/10.1128/MCB.01223-13.
Copyright © 2014, American Society for Microbiology. All Rights Reserved.
doi:10.1128/MCB.01223-13

diplotene stage beginning around E18.5 through the birth of mice (22). After diplotene, oocytes enter a state of prolonged meiosis I arrest, called the dictyate arrest stage. All oocytes reach dictyate arrest by postnatal day 5 (P5) (23). Dictyate-arrested immature oocytes await selection for growth and maturation and eventually ovulation, which first occurs in juvenile stage and also periodically throughout adulthood until menopause (24, 25).

Ironically, while DNA DSBs are known to be the most deleterious form of DNA damage (26), in Spo11 mutant mice, which fail to produce meiotic DNA DSBs, oocytes fail to survive much beyond the birth of mice. Spo11 mice are thereby infertile (27, 28). These facts suggest that an extraordinary level of DNA DSB tolerance during prenatal development is one critical criterion for oocyte survival in postnatal life. It is not known how oocytes withstand such high-level DNA DSBs formed at E14 and during subsequent stages of homologous recombination-mediated DNA repair, which continues up to, or several days beyond, the birth of mice (here called postnatal day 0.5 [P0.5]) (22). In mice that fail to repair meiotic DNA DSBs, the mutant oocytes undergo death and loss after the mice are born (3, 4, 29–33). Thus, the execution of death appears to be delayed for a period of 5 days or more, given DNA DSBs are formed at E14. In comparison, P5 dictyate oocytes undergo death within a single day after relatively weak IR exposure (11). The timing of death of meiotic mutant oocytes appears to coincide with the initiation and rapid increase in TAp63α expression level in oocytes starting from E18.5 up to peak levels by P5 (11). Prior studies have shown that meiotic DNA DSBs and TAp63α expression in oocytes are inversely correlated between E17 to postnatal day 3 (P3) (16), which suggests oocytes may coordinate TAp63α expression with meiotic DNA DSB repair and evade the possibility of undergoing inadvertent death during meiotic DNA DSB repair and recombination. It is easy to presume based on this inverse correlation that oocytes tolerate meiotic or IR-induced DNA DSBs during meiotic DNA DSB formation and repair by virtue of simple absence of TAp63α expression.

In this study, we found that apart from regulating TAp63α expression, oocytes also modulate TAp63α phosphorylation temporally from pre- to postnatal development. Oocytes at first suppress TAp63α phosphorylation induction even upon high-level DNA DSB formation and seem to defy death to help minimize oocyte loss during prenatal meiotic recombination. After meiotic recombination, oocytes are prone to TAp63α phosphorylation induction and death even upon low-level DNA damage, apparently for stringent germ line quality maintenance during postnatal dictyate arrest. Our findings reveal the ATM kinase and a calyculin A (CA)-sensitive Ser/Thr phosphatase are important regulators of TAp63α phosphorylation induction in oocytes upon DNA DSB formation. Based on these findings, we present a model of how the relative balance in kinase and phosphatase activity during pre- to postnatal development may ultimately determine the final level of TAp63α phosphorylation induction and sensitivity of oocytes to meiotic or IR-induced DNA DSBs. Such a model suggests possible alternative strategies to prevent infertility in women who require radiation or chemotherapy treatments.

MATERIALS AND METHODS

Mice, irradiation, and ovary tissue preparation. Timed matings were conducted to stage mice. Male mice were caged together with female mice in the evening and plugs were tested the next day in the morning. Mice on the day of birth were considered P0.5. ICR P0.5, P2, or P5 mice were exposed to whole-body irradiation using a ^{137}Cs gamma irradiator with turntable at the indicated doses, and ovaries were harvested thereafter at different time points for Western blot or immunohistochemistry analyses. Alternatively, ovaries of P0.5 or P5 mice were first dissected, placed briefly in culture medium for chemical treatment, and then irradiated and harvested at indicated doses and time points. Mice on the day of birth were designated P0.5, depending on the precise time of mating and birth, it is estimated that mice designated P0.5 may differ by up to half a day (~12 h) of development between different litters. Animal study protocols used in the present study were approved by the Animal Care Committee of Ewha Womans University.

Chemical treatment of ovaries *in vitro*. P0.5 or P5 ovaries were collected and placed in Waymouth media (Invitrogen) containing 0.23 mM pyruvic acid, 10 μg of streptomycin/ml, 75 μg of penicillin/ml, and 10% fetal bovine serum (HyClone). The ovaries were treated with the phosphatidylinositol 3-kinase (PI3K) inhibitor wortmannin (Merck), the ATM-specific inhibitor KU55933 (Tocris), the DNA-dependent protein kinase catalytic subunit (DNA-PKcs)-specific inhibitor NU7441 (Tocris), or the protein phosphatase 1A and 2A inhibitor calyculin A (Cell Signaling) at the indicated concentrations. The final dimethyl sulfoxide (DMSO) content in final working solutions of chemicals were as follows: wortmannin, 0.3% DMSO; KU55933 or NU7441, 0.1% DMSO; and calyculin A, 0.02% DMSO. Ovaries treated with wortmannin were preincubated for 30 min and then washed out with fresh Waymouth culture medium, followed by ionizing radiation treatment. KU55933-, NU7441-, and calyculin A-pretreated ovaries were preincubated for 2 h, followed by ionizing radiation treatment. Ovaries were harvested at indicated time points for Western blot or immunohistochemistry analyses.

Tissue or cell lysate preparation, Western blotting, and ABC immunoblot sensitivity enhancement. P0.5 or P5 ovaries were thoroughly ground in 50 μl of phosphate-buffered saline (PBS), protease inhibitors, and 1 mM dithiothreitol with a fitted pestle on ice, after which 5× sodium dodecyl sulfate (SDS) loading buffer was added as described previously (11). DNA was sheered by passage through a 1-ml insulin syringe before loading samples on 6, 10, or 15% SDS–PAGE gels to analyze ATM and p63, p63 and tubulin, or γ-H2AX, respectively. SDS-PAGE gels were made from 37.5:1 Protogel acrylamide-bisacrylamide (National Diagnostic, Atlanta, GA) cast in EzWay gel cassettes (10 by 10 by 1.5 cm; KOMA Biotech, Seoul, South Korea), electrophoresed for 140 min, transferred to Protran nitrocellulose (Whatman; GE Healthcare, USA) in EzBlot blotting units (KOMA Biotech) at ca. 25 to 30 mV for 2 h (for p63, tubulin, and γ-H2AX immunoblots) or 13 mV for 16 h. Immunoblots were incubated with primary antibody for 1 h [anti-p63 mouse monoclonal antibody (MAb) 4A4, 1:200 (7); antitubulin mouse MAb AA4.3, 1:1,000 (Developmental Studies Hybridoma Bank, University of Iowa); anti-γ-H2AX(Ser139) rabbit MAb, 1:1,000 (Cell Signaling)] or for 16 h [anti-phospho-ATM(Ser1981) mouse MAb, 1:2,000 (Millipore)]. Secondary antibodies used were either goat anti-mouse IgG conjugated to horseradish peroxidase (HRP; 1:5,000) or goat anti-rabbit IgG–HRP (1:5,000; Jackson ImmunoResearch Laboratories, Inc., West Grove, PA) for 30 min. For avidin-biotin complex (ABC) immunoblot sensitivity enhancement (ATM and DNA-PKcs immunoblots), after primary antibody incubation, immunoblots were washed in PBS–0.1% Tween (PBS-T) and incubated with biotinylated horse anti-mouse IgG secondary antibodies–PBS-T (1:5,000; Jackson ImmunoResearch Laboratories) for 30 min, followed by 30 min of incubation with ABC solution from a Vectastain ABC kit (Vector Laboratories, Burlingame, CA) precomplexed in PBS-T for 30 min prior to use. Immunoblots were washed in PBS–0.1% Tween and developed by using enhanced chemiluminescence.

Immunofluorescence, immunohistochemistry, and quantitation. P0.5 or P5 ovaries were fixed in neutral buffered formalin (Sigma) for 2 h at 4°C. Ovaries were dehydrated through successive changes of 70, 80, 90, and 100% ethanol, 10 min each time, transferred to two changes of xylene, 10 min each time, and then transferred to paraffin (Merck) for 20 min before embedding. Sections (6 μm) were prepared and mounted on

slides. Sections on slides were deparaffinized, boiled in 100 mM citrate buffer (pH 6.0) at 95°C for 30 min, and cooled. For immunofluorescence analyses, the sections were incubated for 1 h with anti-p63 MAb (1:200, 4A4 [7])–1% bovine serum albumin (BSA)–PBS and anti-γ-H2AX(Ser139) rabbit MAb (1:1,000; Cell Signaling), followed by 1% BSA–PBS washes and then Alexa Fluor 568–goat anti-mouse IgG or Alexa Fluor 488–goat anti-rabbit IgG secondary antibodies at 1:200 (Molecular Probes), and counterstained with DAPI (4′,6′-diamidino-2-phenylindole). For immunohistochemistry, the sections were incubated with anti-p63 MAb for 1 h and biotinylated horse anti-mouse IgG secondary antibodies (Jackson ImmunoResearch Laboratories) at 1:200 for 30 min. Sections were further processed using the Vectastain ABC kit (Vector Laboratories) and the DAB peroxidase system (Vector Laboratories). Sections were counterstained with Harris hematoxylin and mounted (Vectamount permanent mounting medium; Vector Laboratories). For γ-H2AX focus analysis, multiple ovary sections were photographed from nonirradiated or irradiated P0.5 and P5 ovaries, and oocytes within an image were digitally cropped using Photoshop and arrayed in order of p63 expression level as measured using ImageJ. γ-H2AX foci were counted from digital images along the ordered array using ImageJ and plotted to comprehensively visualize the overall γ-H2AX focus formation patterns pre- and after IR treatment in p63-expressing versus p63-nonexpressing P0.5 oocyte populations compared to P5 oocytes. To quantify γ-H2AX foci in oocytes, each digitally cropped oocyte in a given section of ovary was saved as a TIFF file and opened in ImageJ. Under the "Process" heading, the "Find Maxima" tool was used. The "Output Type" was set to "Count" function, and the noise tolerance was set to ca. 2 to 3.

To quantify oocyte numbers with or without IR, 6-μm ovary sections were stained with anti-p63 MAb 4A4. Oocytes of primordial follicles and primary or secondary follicles were counted in every fifth section of ovary. The total number of oocytes counted for each ovary was multiplied by 5 to estimate the total number of oocytes per ovary, as described previously (3).

Lentivirus production and 293T cell transduction. Lentiviral expression vectors, which were modified for TAp63α expression, lentiviral production, and transduction as previously described (34), were kindly provided by J.-S. Lee and R. Mulligan (Harvard Gene Therapy Initiative).

RESULTS

Newborn oocytes may initiate TAp63α expression before complete meiotic DNA DSB repair. To investigate the possibility that simple lack of TAp63α expression is the basis for DNA DSB resistance in oocytes during meiotic DNA repair and meiotic recombination, we first examined TAp63α expression and meiotic DNA DSB levels in predictyate newborn oocytes that initiate TAp63α expression at low levels, compared to dictyate P5 oocytes that demonstrate high TAp63α expression. To better perceive a possible inverse correlation between meiotic DNA DSBs and TAp63α expression (16), newborn oocytes within a given section of ovary were numbered and arrayed from low to high TAp63α expression (Fig. 1A; see Fig. S1A in the supplemental material). The number of meiotic DNA DSBs marked by γ-H2AX foci in each arrayed oocyte (Fig. 1A; see also Fig. S1B and S2A and B in the supplemental material) was counted and plotted (Fig. 1B). TAp63α expression was relatively uniform in P5 oocytes (Fig. 1A; see S1A in the supplemental material); thus, they were numbered at random and arrayed (Fig. 1B). In the newborn P0.5 ovary, both oocytes lacking in TAp63α expression and those having TAp63α expression contained γ-H2AX foci (Fig. 1B and C) with TAp63α-lacking oocytes generally containing more γ-H2AX foci than oocytes showing TAp63α expression. Approximately 21% of the P0.5 oocytes contained only γ-H2AX foci and lacked TAp63α expression, ~53% contained only TAp63α expression and lacked γ-H2AX foci, and the remaining ~23% of oocytes contained both TAp63α expression and γ-H2AX foci (Fig. 1D, P0.5). Therefore, meiotic DNA DSB and TAp63α expression levels appeared at some level to be inversely correlated in newborn oocytes but were certainly not mutually exclusive of each other. It was not clear whether newborn oocytes showing overlapping TAp63α expression and γ-H2AX foci were fated for eventual TAp63α-mediated death. Since predominantly all P5 oocytes expressed only TAp63α and lacked γ-H2AX foci (Fig. 1A, B, and D), either all meiotic DNA DSBs underwent repair by P5 dictyate arrest or those which failed to undergo repair underwent TAp63α-mediated death. Increasing the level of DNA DSBs in newborn P0.5 oocytes by IR treatment and assessing the number of oocytes that remain at later stages could determine whether oocytes that incur DNA DSBs undergo DNA repair and survive or undergo death and elimination.

Newborn oocytes tolerate gamma radiation treatment that completely obliterates P5 immature dictyate oocytes. We increased DNA DSB levels in P0.5 and P5 ovaries by 0.45-Gy IR treatment and assessed the number of oocytes that survived up to P7. As before (11), an IR dose of 0.45 Gy eradicated nearly all primordial follicle oocytes in P5 ovaries (Fig. 2A). Only oocytes of growing primary and secondary follicles remained. However, newborn ovaries irradiated with 0.45 Gy of IR and examined at P7 contained numerous primordial follicle oocytes (Fig. 2A and B). Mice born before dusk and examined during the daytime showed ~20% survival, whereas mice born later during the day and examined immediately after birth showed up to 40% primordial follicle oocyte survival (see Fig. S3 in the supplemental material). Western blot analysis also corroborated immunohistochemistry results, which demonstrated the absence of TAp63α signal in P5-irradiated ovaries and the presence of TAp63α signal in P0.5-irradiated ovaries when examined at P7 (Fig. 2C). Therefore, whereas P5 immature primordial follicle oocytes are clearly totally obliterated within only 2 days after IR treatment, a significant number of P0.5 immature oocytes are capable of surviving IR-induced DNA damage for at least 7 days after IR treatment. Primary and secondary follicle oocytes undergoing growth and maturation were also observed in P0.5-irradiated ovaries examined at P7 (Fig. 2A and B; see Fig. S3A and B in the supplemental material). These oocytes probably represent primordial follicle oocytes that survived IR treatment and initiated growth and maturation after irradiation, since no primary and secondary follicle oocytes were present at the time of irradiation. On the other hand, primary or secondary follicle oocytes present in P5-irradiated ovaries at P7 probably represent primary or secondary follicle oocytes already present at the time of irradiation, since folliculogenesis has begun by P5, which survived IR treatment (11).

High doses of gamma radiation treatment fail to induce complete TAp63α phosphorylation in newborn oocytes. Thus far, it was not clear whether P0.5 oocytes lacking in TAp63α expression or oocytes having TAp63α expression survived IR damage. Twenty percent of primordial follicle oocyte survival (Fig. 2B) correlated with oocytes lacking TAp63α expression (Fig. 1D), but we could not rule out the possibility that low-level TAp63α expression in P0.5 oocytes (Fig. 1A; see Fig. S1A in the supplemental material) underlies their capacity to resist DNA damage. Since some P0.5 newborn litters showed >40% of primordial follicle oocyte survival (see Fig. S3 in the supplemental material), a conclusion could not be drawn based solely on correlation. We exam-

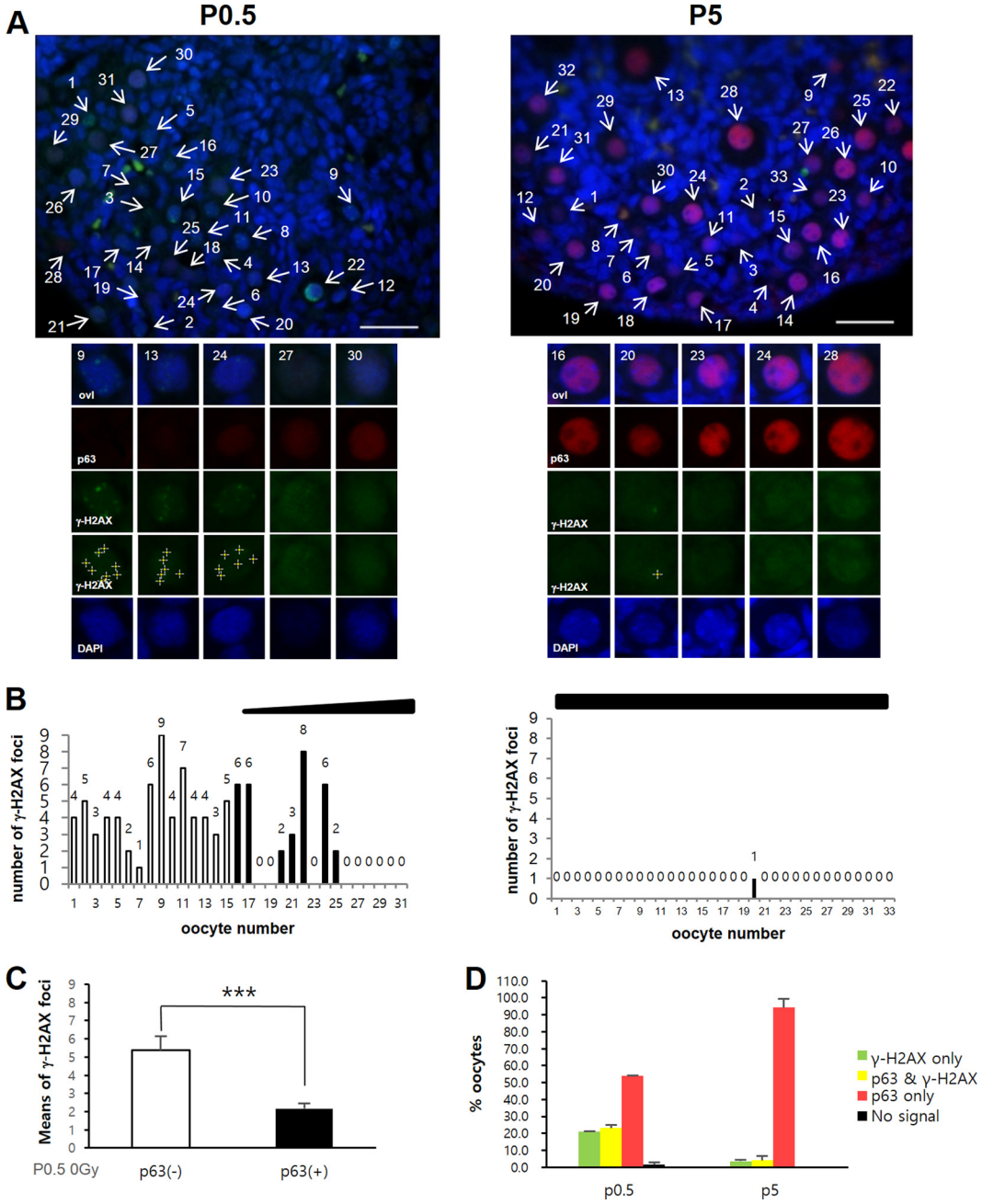

FIG 1 A significant fraction of newborn oocytes initiate TAp63α expression before completing meiotic DNA DSB repair. (A) Representative sections of nonirradiated P0.5 or P5 ovary sections stained for p63 (red), γ-H2AX (green), or DAPI (blue). Images of P0.5 and P5 ovaries were captured using the same camera exposure times. Representative oocytes from the upper panels are enlarged in the lower panels, numbered, and arranged according to TAp63a expression level. Crosses denote γ-H2AX foci counted using ImageJ. See also Fig. S1 in the supplemental material. Scale bars, 50 μm. (B) The numbers of γ-H2AX foci (displayed above the bars) in each oocyte arrayed in panel A and in Fig. S1 in the supplemental material are plotted and displayed. The gradient slope above the plot indicates the relative level of TAp63α expression along the array. Unfilled bars denote numbers of γ-H2AX foci in oocytes lacking in TAp63α expression. Filled bars (or the absence of a bar) denote the numbers of γ-H2AX foci in oocytes with detectable TAp63α expression. (C) Mean numbers of γ-H2AX foci in P0.5 oocytes lacking TAp63α expression [p63(−)] or having TAp63α expression [p63(+)]. $n = 4$ mice; error bars indicate the standard errors of the mean (SEM). ***, $P \leq 0.02$ (Mann-Whitney test). (D) Percent oocytes in P0.5 or P5 ovaries with only γ-H2AX foci, both TAp63α expression and γ-H2AX foci, or only TAp63α expression. Oocytes lacking both signals were nominal. Averages of 141 oocytes (P0.5, 2 mice) or 199 oocytes (P5, 2 mice) were tested; error bars indicate the SEM.

ined whether P0.5 oocytes would induce TAp63α phosphorylation, which is tightly linked with oocyte death (11), as did P5 oocytes upon irradiation. IR-induced TAp63α phosphorylation generates a prominent λ-phosphatase-sensitive electrophoretic mobility shift upon SDS-PAGE (11). Irradiated P5 oocytes clearly showed an IR-induced TAp63α phosphorylation shift, but, interestingly, irradiated P0.5 oocytes did not (Fig. 3A). However, IR-induced γ-H2AX levels increased upon IR treatment in both P0.5

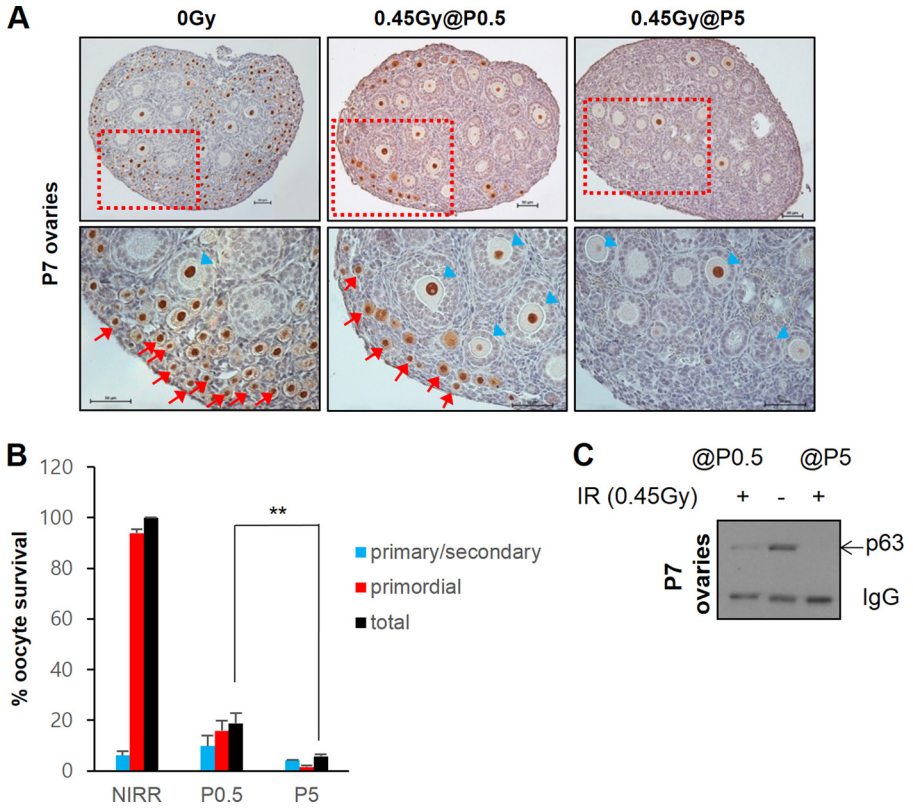

FIG 2 Newborn P0.5 oocytes can resist gamma radiation treatment. (A) The upper panels show representative immunohistochemistry ovary sections stained for p63 of nonirradiated P7 mice (0 Gy) or 0.45-Gy-irradiated P0.5 or P5 mice examined at P7. The lower panels show magnified images of the boxed regions in the upper panels. Arrows, immature primordial follicles oocytes; arrowheads, oocytes undergoing growth and maturation in primary or secondary or follicles. Bars, 50 μm. (B) Quantification of oocyte survival in ovaries of 0.45-Gy-irradiated P0.5 and P5 mice examined at P7 and compared to nonirradiated P7 controls. $n = 3$ mice; error bars indicate the SEM. **, $P \leq 0.002$ (Kruskal-Wallis test). (C) Western blot of TAp63α levels remaining in ovaries of 0.45Gy-irradiated P0.5 versus P5 mice examined at P7 compared to nonirradiated P7 controls. Ovary lysates are equivalent to half of one ovary loaded per lane. IgG, endogenous ovary mouse IgG.

and P5 ovary lysates (Fig. 3B), indicating that DNA damage was certainly incurred in both P0.5 and P5 ovaries upon irradiation. By P2, TAp63α phosphorylation was prominently induced after irradiation (see Fig. S4 in the supplemental material) but a small fraction remained incompletely shifted. Therefore, it appeared that oocytes quickly acquire the potential to induce TAp63α phosphorylation after birth.

To determine whether a higher dose of IR would suffice to induce TAp63α phosphorylation, a pair of contralateral P0.5 ovaries were dissected, and one was irradiated with 20 Gy, while the other served as the nonirradiated control. Although a 20-Gy IR dose is >100-fold over the minimum threshold dose of 0.1 to 0.2 Gy required for inducing TAp63α phosphorylation in P5 oocytes (11) (see also Fig. 6D), P0.5 oocytes induced TAp63α phosphorylation only partially after a 20-Gy IR treatment (Fig. 3C). To rule out the possibility that placing ovaries in culture media hampered more complete TAp63α phosphorylation induction, P0.5 ovaries were irradiated *in vivo* by exposing mice to 20 Gy of whole-body IR, and ovaries were taken for immunoblot analysis 2 h later when mice remained viable. The *in vivo*-irradiated ovaries also failed to induce high-shift TAp63α phosphorylation (Fig. 3D). Whether ovaries were irradiated *in vitro* or *in vivo*, P0.5 mice were clearly deficient in IR-induced TAp63α phosphorylation (see Fig. S5 in the supplemental material). Differences in the level of TAp63α phosphorylation induced by IR appear to be related to differences in the developmental progression rates of mice of different litters (with more developmentally advanced mice showing higher levels of TAp63α phosphorylation) rather than differences in irradiation conditions (*in vivo* versus *in vitro*) (see Fig. 6). Interestingly, although a high-shift TAp63α band was absent upon IR at 20 Gy (Fig. 3D), a low-shift band above baseline unshifted TAp63α was clearly induced (Fig. 3D, single arrowhead), which also appeared in earlier P0.5-irradiated ovary (Fig. 3C, single arrowhead). Tubulin bands on the same immunoblot showed no electrophoretic mobility shift (Fig. 3D). The nature of the modification generating low-shift TAp63α was not yet clear. Later experiments suggested the low-shift band was also induced by a phosphorylation modification (see Fig. S9 in the supplemental material), and thus the degree of TAp63α shift above baseline appears to indicate the degree of compound phosphorylation. In summary, newborn oocytes showed a clear deficiency in inducing TAp63α phosphorylation whether irradiated *in vitro* or *in vivo* and induced at best TAp63α phosphorylation partially after treatment with >100-fold above the minimum 0.1- to 0.2-Gy threshold dose for inducing TAp63α phosphorylation in P5 oocytes (11) (see Fig. 6). Thus, newborn oocytes lacked IR-induced TAp63α phosphorylation, formerly shown to be tightly linked with IR-induced oocyte death (11).

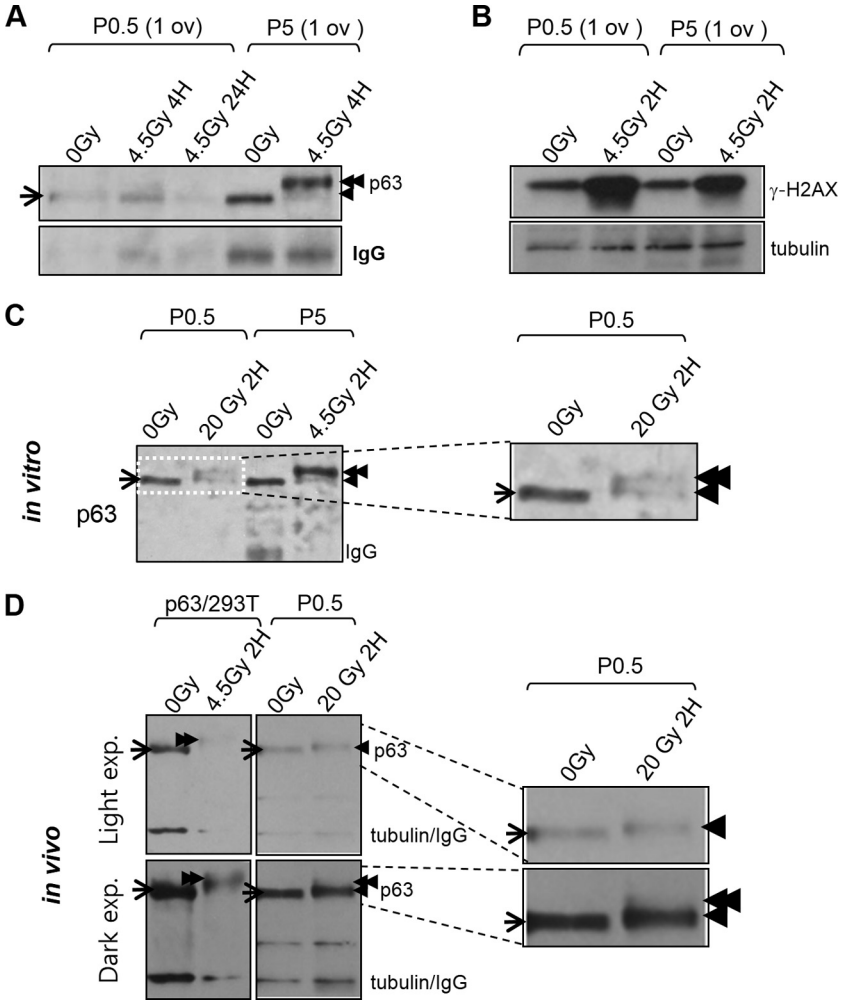

FIG 3 Newborn P0.5 oocytes are TAp63α phosphorylation deficient even after high-dose IR treatment. (A) Immunoblot of TAp63α phosphorylation shift in ovary lysates from nonirradiated versus 4.5-Gy-irradiated P0.5 versus P5 mice at the indicated time points after IR treatment. Lysate of one ovary loaded per lane. Arrow, baseline nonshifted TAp63α; single arrowhead, low shift; double arrowhead, high shift. IgG, endogenous mouse ovary IgG. (B) Immunoblot levels of γ-H2AX in contralateral nonirradiated versus 4.5-Gy-irradiated dissected ovaries of P0.5 and P5 mice at 2 h after IR treatment. (C) Immunoblot of TAp63α phosphorylation shift levels in nonirradiated versus high-dose, 20-Gy-irradiated dissected contralateral newborn ovaries compared to nonirradiated versus 4.5-Gy-irradiated P5 ovaries examined 2 h after IR treatment. Endogenous ovary IgG washes away during a 2-h post-IR incubation period in culture. The boxed region magnified at the right. Arrows and arrowheads are as described for panel A. (D) Immunoblot of TAp63α phosphorylation shift induction in ovaries of newborn mice exposed to whole-body 20-Gy IR 2 h after treatment (magnified at the right). For comparison, TAp63α phosphorylation shifts in lysates of 0-Gy-irradiated versus 4.5-Gy-irradiated TAp63α lentivirus-transduced 293T cells loaded in adjacent lanes are also shown. Arrows and arrowheads are as described for panel A. Light film exposure reveals low-shift TAp63α. Dark film exposure reveals a faint trace of high-shift TAp63α.

Chemical inhibition of ATM activity blocks IR-induced TAp63α phosphorylation and prevents oocyte death. Given the lack of TAp63α phosphorylation in newborn oocytes, which also survive IR-induced DNA damage (Fig. 2 and 3), we sought to examine whether TAp63α phosphorylation is actually required for IR-induced oocyte death. The ATM kinase is a central kinase in the DNA damage response that transduces DNA damage signaling to downstream target proteins, including p53 and H2AX, by phosphorylation commonly at S/TQ motifs (35–38). Previously, we found mutagenesis of S/TQ sites within the C-terminal domain of TAp63α significantly reduced IR-induced TAp63α phosphorylation shift in transduced 293T cells (39). Furthermore, treating TAp63α lentivirus-transduced 293T cells with wortmannin, an inhibitor of PI3K-like kinase family, which includes ATM, ATR, and DNA-PKcs (40), effectively blocked IR-induced TAp63α phosphorylation shift. Together, these results suggested that IR-induced TAp63α phosphorylation depends on ATM activity (39).

In P5 ovaries, we found wortmannin or ATM-specific inhibitor KU55933 treatment strongly blocked IR-induced ATM Ser1981 autophosphorylation (41), a widely used indicator of ATM activation, and completely inhibited TAp63α phosphorylation induction (Fig. 4A; see Fig. S6A in the supplemental material). Lower concentrations of KU55933 ATM inhibitor effectively blocked TAp63α phosphorylation induction in TAp63α lentivirus-transduced 293T cells (see Fig. S6B in the supplemental material), probably due to more effective chemical penetration into cultured cells than into the ovary. High concentrations of the DNA-PKcs inhibitor NU7441 failed to block both ATM Ser1981 phosphorylation and TAp63α phosphorylation in both TAp63α-transduced 293T cells (see Fig. S6B in the supplemental material)

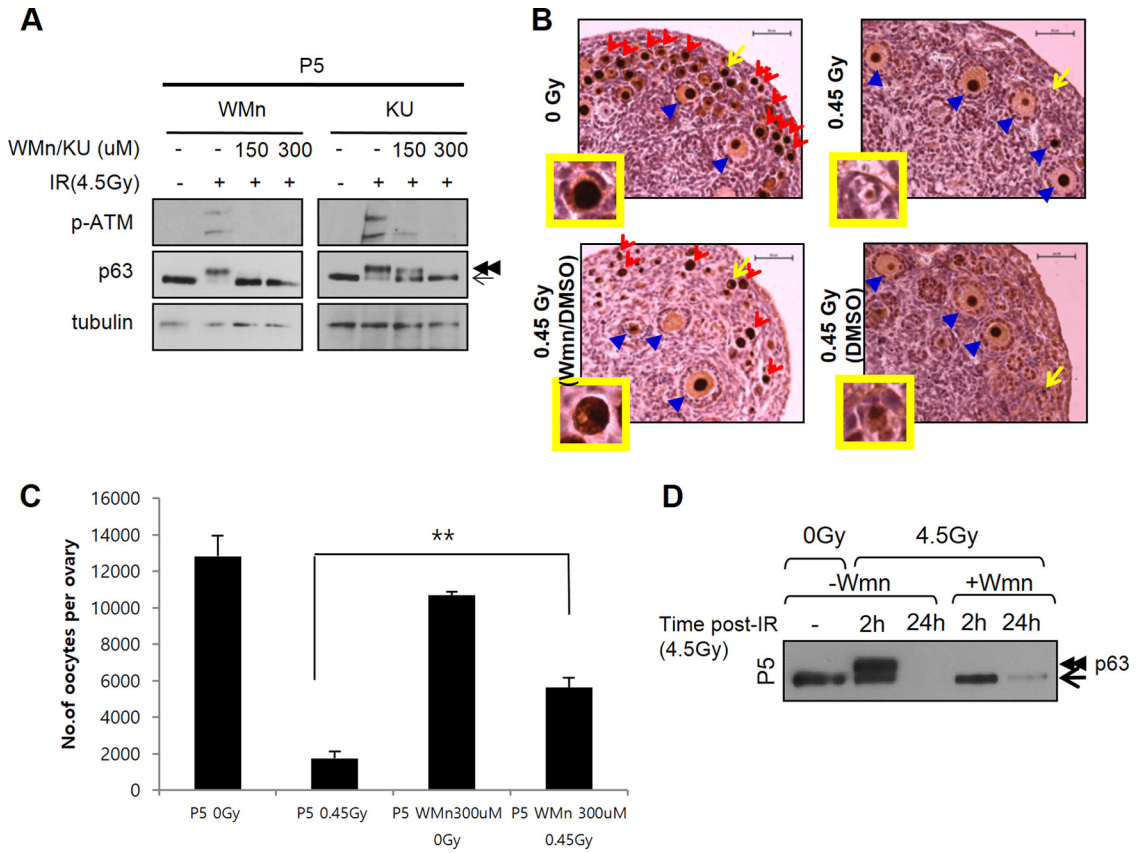

FIG 4 PI3K-like kinase inhibitor wortmannin and ATM inhibitor KU55933 block IR-induced TAp63α phosphorylation and IR-induced primordial follicle oocyte death. (A) Immunoblots showing the levels of ATM Ser1981phosphorylation using phospho-specific MAb (upper panels) and TAp63α phosphorylation shift (middle panels) in nonirradiated or 4.5-Gy-irradiated P5 ovaries without or with wortmannin (WMn) or KU55933 (KU) pretreatments using the indicated doses. Wortmannin pretreatments were for 30 min on dissected ovaries, followed by washing before IR treatment. KU55933 pretreatments were for 2 h prior to IR treatment. Ovaries were examined 2 h after IR treatment. Contralateral ovary pairs, denoted by brackets, were used and loaded adjacently. Arrow, nonshifted TAp63α; double arrowheads, high shift. Tubulin, loading control. (B) Immunohistochemistry sections of nonirradiated versus 0.45-Gy-irradiated P5 ovaries examined at P7. Ovaries were either untreated or pretreated with wortmannin in DMSO (Wmn/DMSO) or pretreated with only DMSO (DMSO) as outlined for 30 min, washed, and irradiated. The ovaries were examined at P7. Red arrowheads indicate primordial follicle oocytes; blue arrowheads indicate primary or secondary follicle oocytes undergoing growth and maturation; the arrows point to representative oocytes magnified in the insets. Scale bars, 50 μm. (C) Quantification of total number of oocytes in P5 ovaries treated as outlined. Ovaries were examined 2 days after IR treatment at P7 ($n = 3$ mice); error bars indicate the SEM. **, $P \leq 0.002$ (Kruskal-Wallis test). (D) Immunoblots analysis of TAp63α levels remaining, which is indicative of oocyte survival, in nonirradiated or 4.5-Gy-irradiated ovaries without (−Wmn) or with (+Wmn) wortmannin pretreatment 2 or 24 h after IR treatment, as outlined.

and P5 oocytes (see Fig. S6C in the supplemental material). In all, these results suggested ATM activity, rather than DNA-PKcs activity, is required for IR-induced TAp63α phosphorylation. Whether ATM directly or indirectly mediates TAp63α phosphorylation requires further study.

Having found a means of blocking TAp63α phosphorylation induction, we next examined whether TAp63α phosphorylation is required for oocyte death. As before, P5 ovaries not pretreated with chemicals or pretreated with 0.3% DMSO and irradiated with 0.45 Gy of IR contained no viable primordial follicle oocytes (Fig. 4B, right panels). Only primary and secondary follicle oocytes undergoing growth and maturation survived. However, wortmannin–0.3% DMSO-pretreated P5 ovaries irradiated with 0.45 Gy of IR contained both numerous primordial follicle oocytes and oocytes undergoing growth and maturation (Fig. 4B, lower left panel). Immunoblot analysis corroborated immunohistochemistry results showing that TAp63α was not detectable in irradiated ovaries not treated with wortmannin but was detectable in wortmannin-pretreated and irradiated ovaries (Fig. 4D, compare lanes 3 and 5). Therefore, TAp63α phosphorylation induction is important for oocyte death induction. These results suggested that the deficiency in TAp63α phosphorylation induction in newborn P0.5 oocytes (Fig. 3) at least in part accounts for their ability to survive IR damage (Fig. 2).

Newborn oocytes induce weak γ-H2AX focus formation after gamma radiation treatment. It is conceivable that differences in IR-induced TAp63α phosphorylation induction levels in P0.5 and P5 oocytes could be due to possible differences in ATM kinase activity. Phospho-specific ATM Ser1981 MAb antibody failed to recognize antigen by immunohistochemistry, which precluded comparison of ATM activity in oocytes by this method (data not shown). Furthermore, follicle cells, which greatly outnumber oocytes in the ovary, also appear to activate ATM Ser1981 phosphorylation upon IR treatment (see Fig. S7 in the supplemental material), making a reliable comparison by immunoblot experiments of whole-ovary lysates improbable. Since ATM is known to mediate H2AX phosphorylation at Ser139, forming γ-H2AX, which binds and forms foci at DNA DSB sites (37, 42), we sought

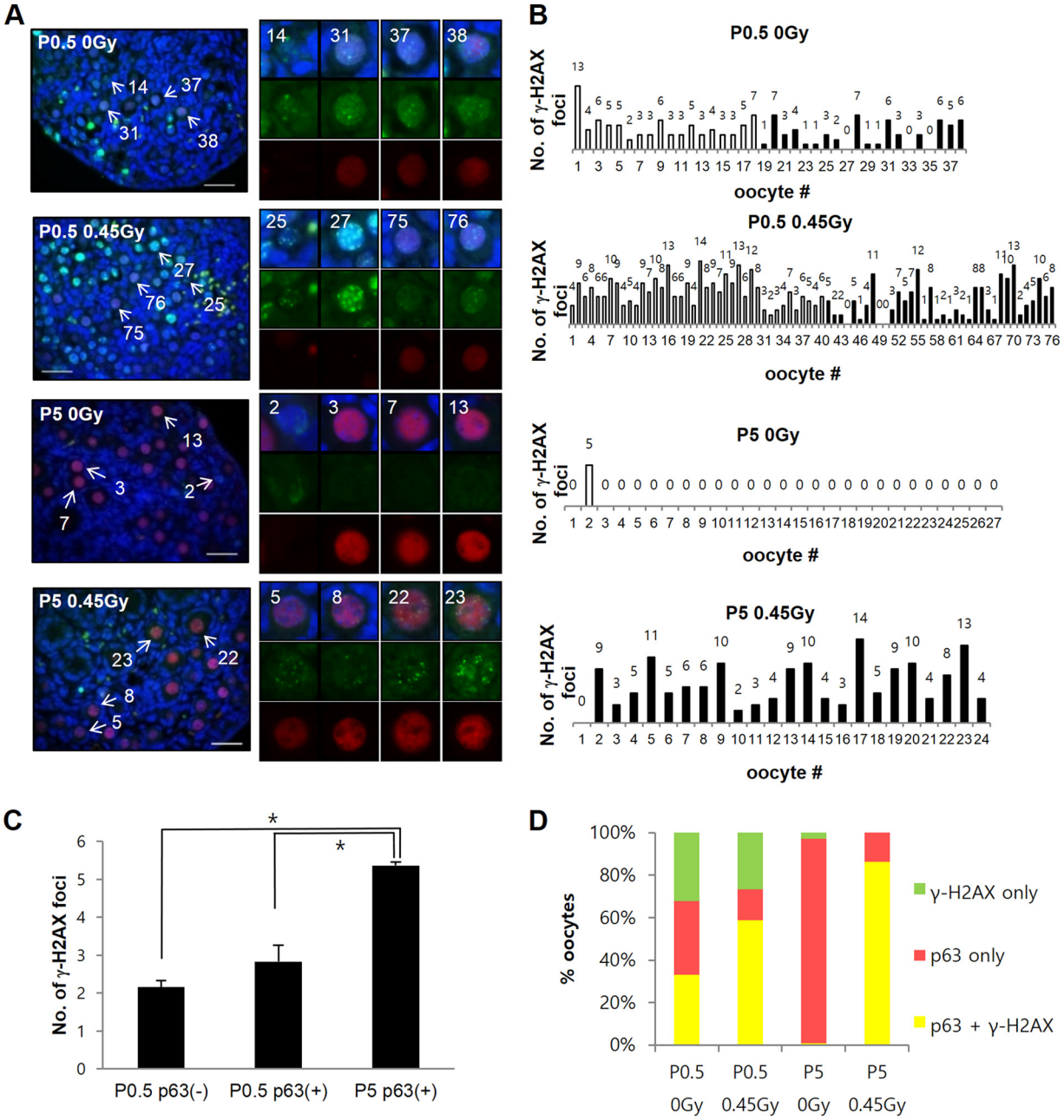

FIG 5 Newborn P0.5 oocytes induce weak γ-H2AX focus formation compared to P5 oocytes after IR treatment. (A) Representative immunofluorescence sections of P0.5 or P5 ovaries either not irradiated or irradiated with 0.45 Gy of IR and stained for p63 (red), γ-H2AX PAb (green), and DAPI (blue) 2 h after IR treatment. The oocytes are numbered according to the level of TAp63α expression, as described in Fig. 1. The indicated oocytes are magnified on the right. Bars, 50 μm. (B) Plot showing the number of γ-H2AX foci in oocytes of ovary sections shown at left arrayed from low to high TAp63α expression, as described in Fig. 1. (C) The average numbers of γ-H2AX foci increased in P0.5 oocytes lacking TAp63α expression [P0.5 p63(−)] or containing TAp63α expression [P0.5 p63(+)] or P5 oocytes, which all contain TAp63α expression [P5 p63(+)] 2 h after 0.45-Gy IR treatment. $n = 2$ mice for each P0.5 and P5 condition; error bars indicate the SEM. *, $P < 0.05$ (Kruskal-Wallis test). The numbers of oocytes were as follows: P0.5, 0 Gy, 133; P0.5, 0.45 Gy, 192; P5, 0 Gy, 50; and P5, 0.45 Gy, 44. (D) Percent oocytes in nonirradiated or irradiated P0.5 versus P5 ovaries analyzed in panel C containing γ-H2AX only (green fraction), TAp63α only (red fraction), or both γ-H2AX and TAp63α (yellow fraction).

to examine γ-H2AX focus formation in oocytes by immunofluorescence as one possible indirect measure of ATM kinase activity. Earlier results showed by immunoblotting that γ-H2AX levels increase in both P0.5 and P5 ovary lysates (Fig. 2B), but the increase may not reflect specific change in oocytes, which required examination by immunofluorescence (Fig. 5A). Although both P0.5 and P5 oocytes increased γ-H2AX focus numbers after irradiation (see Fig. S8 in the supplemental material), the level of increase appeared to be less striking in P0.5 oocytes than in P5 oocytes (Fig. 5B). TAp63α-lacking and TAp63α-expressing P0.5 oocyte fractions both showed an increase in γ-H2AX focus formation after irradiation (see Fig. S8 in the supplemental material) that aver-

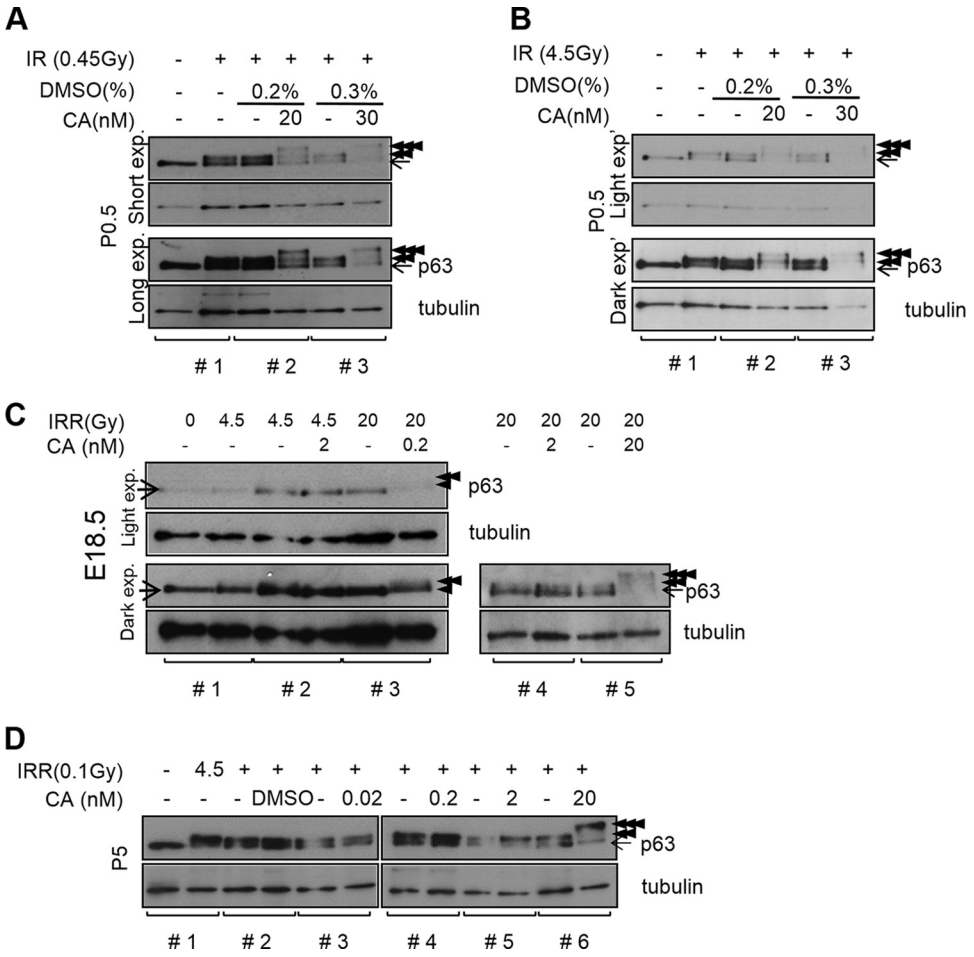

FIG 6 Calyculin A (CA)-sensitive Ser/Thr protein phosphatase downregulates IR-induced TAp63α phosphorylation in predictyate P0.5 oocytes. (A and B) Immunoblots showing the level of IR-induced TAp63α phosphorylation in nonirradiated (−), 0.45-Gy-irradiated (A), or 4.5-Gy-irradiated (B) newborn ovaries pretreated with DMSO and CA at indicated concentrations. Ovaries were examined 2 h after IR treatment. In each immunoblot, brackets mark contralateral ovaries pairs from littermate mice. Tubulin, loading control. Arrow, nonshifted TAp63α; double arrowheads, high shift; triple arrowheads, superhigh shift. Upper two panels, short exposure; lower two panels, long exposure. (C) IR-induced TAp63α phosphorylation in contralateral (brackets) E18.5 ovaries without or with CA pretreatment, followed by IR treatment at the indicated doses. Ovaries were examined 2 h after IR treatment. Arrows and arrowheads are as described in panel A. (D) TAp63α phosphorylation induction in contralateral ovaries of P5 mice not irradiated or irradiated with subthreshold 0.1-Gy IR without or with CA pretreatment as indicated and examined 2 h after IR treatment.

aged ~2.1 and ~2.8 foci per oocyte (Fig. 5C), respectively. P5 oocytes induced a higher average of ~5.5 foci per oocyte in parallel experiments (Fig. 5C). Furthermore, when comparing the percent TAp63α-expressing P0.5 versus P5 oocytes that increase γ-H2AX upon IR treatment, a 2-fold increase, from 30 to 60%, occurred in P0.5 ovaries, whereas in P5 oocytes the increase was considerably greater, from <1 to 85% (Fig. 5D, yellow bars). Therefore, there were clear measurable differences in γ-H2AX induction levels between P0.5 and P5 oocytes. The lack of TAp63α phosphorylation induction in P0.5 oocytes could be an outcome of weak ATM kinase activity or, more generally, an overall weak DNA damage response activation in P0.5 oocytes compared to P5 oocytes.

A calyculin A-sensitive Ser/Thr protein phosphatase downregulates IR-induced TAp63α phosphorylation in both newborn and P5 dictyate oocytes. We next sought to examine other possible causes for the lack of TAp63α phosphorylation induction in newborn oocytes. Phosphatases have emerged as important modulators of DNA damage response activation (43), which led us to question whether protein phosphatases may be culpable for the deficiency in IR-induced TAp63α phosphorylation in P0.5 oocytes. Calyculin A (CA) is a potent inhibitor of PP1 and PP2 Ser/Thr protein phosphatases, which accounts for reportedly >95% phosphatase activity in cells (44). We tested whether blocking Ser/Thr phosphatase activity with CA might facilitate IR-induced TAp63α phosphorylation in P0.5 oocytes. Without CA pretreatment or with mock DMSO-only pretreatment, we observed that TAp63α phosphorylation was partially shifted by 0.45-Gy (Fig. 6A) and 4.5-Gy (Fig. 6B) IR treatments. Thus, TAp63α phosphorylation induction was deficient in newborn P0.5 oocytes (Fig. 6A and B), as suggested earlier (Fig. 3). Differences in the degree of deficiency appear to arise from different developmental progression rates of mice in different litters. We noticed that mouse litters that were birthed during the day and analyzed immediately after birth showed weaker TAp63α phosphorylation induction than mice that were born earlier, before dusk, and analyzed later, which

showed partial TAp63α phosphorylation induction. Overall, oocytes of developmentally younger mice (Fig. 3A, P0.5 oocytes; Fig. 6C, E18.5 oocytes) appear to have weaker potential to induce TAp63α phosphorylation than the oocytes of older mice (see Fig. S4 in the supplemental material, P2 oocytes; Fig. 3A and 6D, P5 oocytes). The P0.5 developmental stage appears to be the fulcrum point when the switchover in TAp63α phosphorylation-inducing potential occurs. The variable level of TAp63α phosphorylation deficiency in newborn P0.5 mice may also arise from experimental factors that are difficult to control more precisely. We estimate newborn mice of different litters could differ developmentally by up to half a day depending on factors, such as the actual time of conception and birth of mice, resulting in differences in TAp63α phosphorylation levels. Despite some variability, we observed that all newborn oocytes were TAp63α phosphorylation deficient and that 0.45 and 4.5 Gy of IR were subthreshold IR doses that induced TAp63α phosphorylation only partially (Fig. 6A and B). Ovaries from mice of the same litter showed nearly the same level of phosphorylation deficiency (Fig. 6A and B; see Fig. S5 in the supplemental material), although we found a rare instance when one mouse appeared to be significantly more phosphorylation deficient than littermates (see Fig. S9A, mouse 3, in the supplemental material). Therefore, all subsequent experiments were conducted with ovaries from littermate mice (Fig. 6; see Fig. S9 and S10 in the supplemental material).

Upon CA pretreatment, we observed 20 nM CA induced a superhigh-shift TAp63α band upon treatment with 0.45 and 4.5 Gy of IR (Fig. 6A and B); this band appeared to be sensitive to both ATM kinase inhibitor KU55933 and λ-phosphatase treatments (see Fig. S9A and B in the supplemental material). Thus, high- and superhigh-shift TAp63α bands appeared to be phosphorylation modifications mediated by ATM (Fig. 6A and B; see Fig. S9A and B, double and triple arrowheads, respectively, in the supplemental material). Also, the low-shift phosphorylation apparent in P0.5 ovaries that induced TAp63α shifts partially (Fig. 3C; see Fig. S9C, single arrowhead, in the supplemental material) was also blocked by inhibitors of ATM. Thus, low, high, and superhigh TAp63α shifts all may be compound ATM-mediated phosphorylations. CA treatment alone without IR did not induce an appreciable TAp63α phosphorylation shift, except for a faint trace in P0.5 oocytes, possibly induced by endogenous meiotic DNA DSBs (see Fig. S10 in the supplemental material).

Interestingly, a fraction of TAp63α remained unshifted after irradiation even with CA pretreatment (Fig. 6A and B). Raising the CA pretreatment dose to 30 nM, followed by irradiation, reduced the overall TAp63α levels (Fig. 6A and B), perhaps due to toxicity at the higher dose combined with IR treatment. Therefore, 20 nM CA appeared to be the maximum effective dose for Ser/Thr phosphatase inhibition. Although this result implied that other protein phosphatases insensitive to CA might also downregulate TAp63α phosphorylation, we found this scenario unlikely because it would require separate pools of TAp63α, each subject to separate regulation by phosphatases following the same IR stimulus. The mechanisms required to maintain such separate TAp63α pools within one nuclear compartment may be unduly complex, which led us to consider that other mechanisms might be involved.

The P0.5 ovary contains a heterogeneous group of oocytes, based on differences in γ-H2AX-marked meiotic DNA DSB and TAp63α expression levels between oocytes (Fig. 1A and B; Fig. 5A and B). Since IR-induced TAp63α phosphorylation shifts examined by immunoblotting represent an average of all oocytes in the P0.5 ovary, different oocytes within the newborn ovary may have different phosphorylation potential. Based on the fact that IR-induced TAp63α phosphorylation was more strongly induced in older P2 and P5 oocytes than younger newborn P0.5 oocytes (Fig. 3; see Fig. S4 in the supplemental material), we predicted that still younger E18.5 oocytes would have even less TAp63α phosphorylation-inducing potential than 1-day-older newborn P0.5 oocytes. When tested, indeed, E18.5 oocytes did not induce TAp63α phosphorylation after a 4.5-Gy IR treatment (Fig. 6C). They induced only a very moderate level of IR-induced TAp63α phosphorylation after a high-dose 20-Gy IR treatment. These results confirmed that progressively younger oocytes were indeed more recalcitrant in TAp63α phosphorylation induction. Therefore, in P0.5 mice that show partial TAp63α phosphorylation upon 0.45 or 4.5 Gy of IR treatment (Fig. 6A and B), a fraction of the oocytes may be developmentally closer to E18.5 and thereby fail to induce TAp63α phosphorylation, while the other fraction that does induce phosphorylation may be developmentally closer to P1. Likewise, newborn oocytes that seem to completely lack TAp63α phosphorylation induction after IR treatment (Fig. 3A; see Fig. S7B and D in the supplemental material) may be developmentally closer to E18.5. Inhibiting Ser/Thr phosphatase activity with 20 nM CA and treatment with high-dose 20-Gy IR induced a TAp63α phosphorylation shift (Fig. 6C) and left little trace of an unshifted fraction. Therefore, numerous phosphatases need not be invoked in the mechanism of TAp63α phosphorylation downregulation. Inhibiting a single class of Ser/Thr phosphatases with CA sufficed to induce nearly complete TAp63α phosphorylation shift given sufficiently high-threshold IR damage (Fig. 6C).

Given that P5 oocytes have high TAp63α phosphorylation potential, we next sought to determine whether Ser/Thr phosphatase activity is lost by the dictyate arrest stage. P5 ovaries pretreated with 20 nM CA and irradiated with a subthreshold 0.1-Gy dose induced superhigh-shift TAp63α phosphorylation (Fig. 6D, triple arrowheads). Thus, Ser/Thr phosphatase activity was in fact present and active in P5 oocytes. Nevertheless, P5 oocytes can induce TAp63α phosphorylation following much lower doses of IR than those observed in newborn oocytes. Therefore, TAp63α phosphorylation-downregulating Ser/Thr phosphatase activity is somehow effectively overcome in dictyate P5 oocytes but not in predictyate stage E18.5 and newborn oocytes. Given that E18.5, P0.5, and P5 oocytes all required the same 20 nM CA dose to facilitate TAp63α phosphorylation, phosphatase activity appears to be constant during this period, indicating that kinase activity is the variable that must change.

DISCUSSION

Meiotic recombination is a hallmark of germ cells required for genetic diversification of gametes. Although the great majority of oocytes generated during embryogenesis undergo death during this period, more than a million oocytes in humans (1), or approximately ten thousand in mice (3), survive the onslaught of Spo11-induced DNA DSBs and successfully complete meiotic recombination such that oocyte numbers are sufficient and plentiful to support fertility in adulthood. It is easy to speculate that delayed onset of TAp63α expression at E18.5, which is well after meiotic DNA DSB formation at E14 (Fig. 7A), may allow sufficient time for DNA DSB repair such that oocytes evade the possibility of TAp63α-mediated oocyte death during prophase I leptotene and

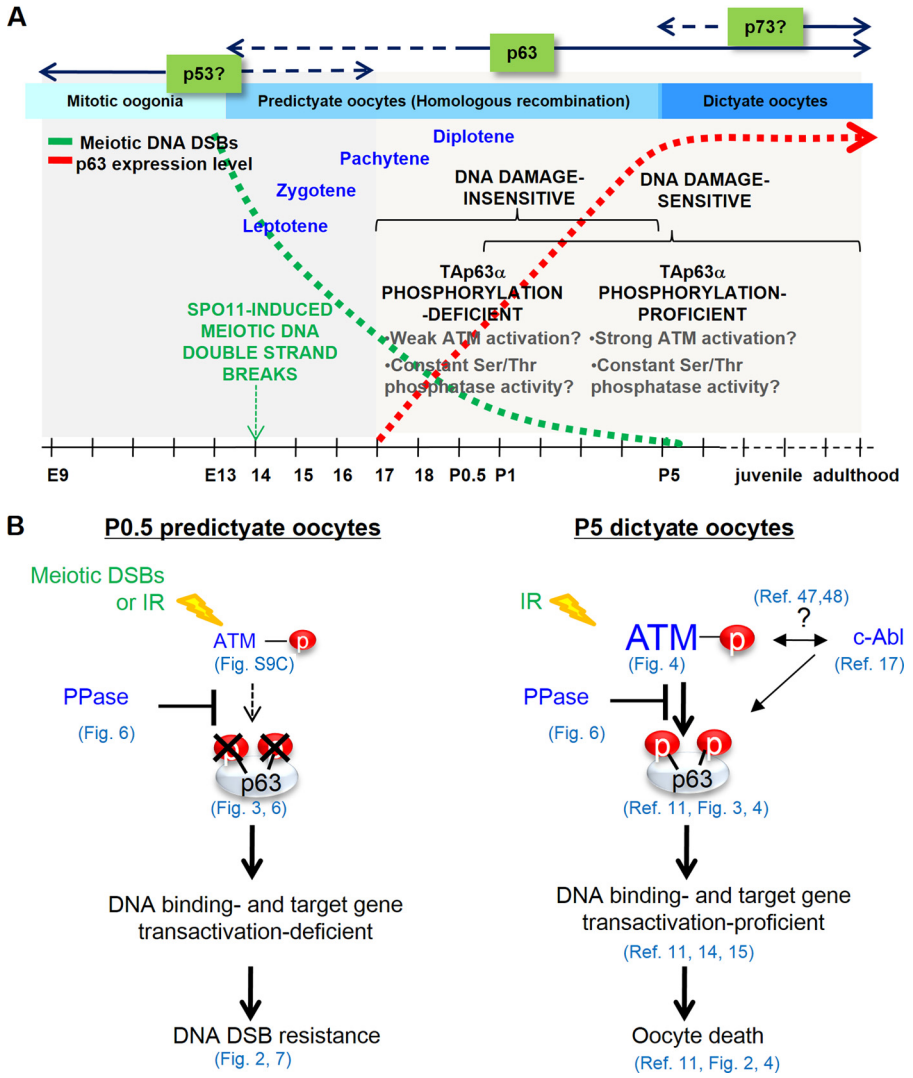

FIG 7 Summary and model of TAp63α expression and phosphorylation regulation and DNA damage sensitivity changes during oocyte development. (A) Timeline outlining the increase in TAp63α phosphorylation potential and DNA damage sensitivity in oocytes in the context of prophase I events during female germ line development. Meiotic DNA DSB levels decline (green dotted line) through homologous recombination-mediated DNA repair as TAp63α expression levels rise in oocytes (red dotted line), starting from E18.5 and peaking at P5. Note that the "DNA damage-sensitive" and "DNA damage-insensitive" refer to only immature primordial follicle oocytes. (B) Model showing how relative activities of the p63 phosphorylation ATM kinase and TAp63α phosphorylation downregulating Ser/Thr protein phosphatase (PPase) in P0.5 versus P5 oocytes could determine the final level of TAp63α phosphorylation induction and oocyte survival or death upon meiotic or IR-induced DNA DSB formation.

zygotene stages of meiotic recombination. Apart from regulated TAp63α expression, the present findings suggest that regulated TAp63α phosphorylation during oocyte development (Fig. 7A) is also a survival mechanism that allows young oocytes undergoing meiotic recombination a measure of protection from meiotic DNA DSBs. E18.5 and P0.5 oocytes are deficient in inducing IR-induced TAp63α phosphorylation (Fig. 3, 6, and 7), which is required for death induction (Fig. 4). The calyculin A-sensitive Ser/Thr protein phosphatase that downregulates TAp63α phosphorylation appears to only partly explain the deficiency in newborn oocytes. It does not explain why progressively younger oocytes require much higher doses of IR to undergo phosphorylation or why P5 oocytes that also harbor CA-sensitive phosphatase activity easily induce TAp63α phosphorylation after very low doses of IR treatment (Fig. 6). Differences in ATM kinase activity between young and older oocytes could be one variable underlying differences in TAp63α phosphorylation induction. Changes in ATM activity have been described in mature meiotically competent oocytes (45). Reduced levels of γ-H2AX focus formation after irradiation in P0.5 oocytes compared to P5 oocytes (Fig. 5) may be an indication of differential ATM activity between immature P0.5 and P5 oocytes. However, one caveat is that H2AX Ser139 phosphorylation has been shown to form independently of ATM kinase activity at least in spermatocytes (46). Therefore, possible differences in ATM activity between newborn predictyate and P5 dictyate oocytes require more certain verification.

Although the present study implicates ATM in mediating TAp63α phosphorylation and oocyte death, it is not clear whether TAp63α is a direct or indirect target of the ATM kinase. Previous studies have implicated the c-Abl tyrosine kinase in mediating

TAp63α phosphorylation and oocyte death upon cisplatin-induced DNA damage (17). However, others have directly challenged this initial report (19, 20). Studies in somatic cell lines showed that ATM activates c-Abl (47) and, more recently, that c-Abl activates ATM (48), which suggests the possibility of functional synergy of these two kinases in activating oocyte death upon DNA damage (Fig. 7B). However, this straightforward conclusion is somewhat confounded by earlier studies in *Caenorhabditis elegans*, which showed that c-Abl deletion mutants or wild-type worms treated with an c-Abl inhibitor, imatinib, render oocytes more sensitive, rather than resistant, to cisplatin treatment (49). Further studies are necessary to help clarify these discrepancies. Also, we do not yet know whether the Ser/Thr protein phosphatase directly dephosphorylates TAp63α or acts on upstream factors, such as possibly the ATM kinase. Interestingly, recent studies in *C. elegans* have shown that loss of function of the dual-specificity phosphatase, LIP-1, sensitizes germ cells to IR-induced and p53 (Cep-1)-dependent death (50). Therefore, phosphatases appear to negatively regulate p53/Cep-1 function, but there is as yet no compelling evidence to suggest that p53/Cep-1 is the direct LIP-1 target. We also observed IR induced low-, high-, and super-high-shift ATM-mediated TAp63α phosphorylation (Fig. 3D and 6; see also Fig. S9 in the supplemental material) that were separable by SDS-PAGE, but their respective molecular functions are not known.

Other members of the p53 family, including p53 itself and TAp73, have been shown to play some part in female germ line maintenance (12, 51). Whether these factors function together or independently at different stages of oocyte development is open to question. We failed to detect TAp73 expression in dictyate oocytes by both immunohistochemistry and immunoblotting with antibodies that picked up endogenous TAp73 expression in the neuroblastoma cell line MCiX-C (data not shown). However, others have reported some level of variable nuclear and cytoplasmic staining in postnatal mouse oocytes (51), and genetic deletion of TAp73 was found to affect the formation of normal spindle bodies in ovulated oocytes (52). Therefore, it is possible that TAp73 functions in late stages during oocyte growth and maturation (Fig. 7A) in the spindle assembly checkpoint (52), when TAp63α levels decline (11). p53 appears to be nonessential for IR-induced oocyte death in dictyate stage oocytes of mice (11). However, *Drosophila* studies showed that p53 is activated by Spo11-induced meiotic DNA DSBs in early-prophase I oocytes, and loss of p53 function resulted in reduced meiotic recombination frequencies (53). Thus, p53 in mice may be dispensable in dictyate stage oocytes but important in early-prophase I meiotic oocytes for meiotic recombination (Fig. 7A).

Interestingly, germ line maintenance in *Drosophila* and *C. elegans* depends on a single existing p53 gene product that functions from early to late prophase I (53–55). Diversification of the p53 gene in higher vertebrates may have allowed three different members—p53, p63, and p73—to adopt specialized roles for specific stages of germ line development (Fig. 7A), possibly for optimized meiotic recombination and germ line quality maintenance. How might functional specialization of p53 family members achieve germ line optimization? The answer may lie in the perhaps different sensitivities of each p53 member to DNA damage. Since TAp63α may be activated by merely 0.3 Gy of IR (11), it may be unsuitable or actually deleterious if it were to be expressed in early prophase I, when hundreds of Spo11-induced meiotic DNA DSBs form. p53 may be more suitable at this stage, because it appears to be less sensitive to DNA damage, given that IR doses ranging between 5 and 20 Gy are typically used to activate p53 (56, 57). Therefore, p53 may function to promote meiotic recombination in the presence of Spo11-induced DNA DSB formation without activating oocyte death. Likewise, mammalian p53 may serve inadequately in dictyate stage oocytes, because exceptionally high-quality germ line maintenance requires stringent culling mechanisms and factors that are highly responsive to low levels of DNA damage, which may only be proffered by factors such as TAp63α due to structural protein differences that are encoded in the gene. According to this model, because *C. elegans* and *Drosophila* have a single p53 gene that must carry out all of the roles executed by p53, p63, and p73 in higher vertebrates, invertebrate p53 must compromise the stringency of germ line culling to accommodate p53 function in Spo11-induced meiotic recombination. Indeed, extremely high IR doses ranging between 40 and 100 Gy are necessary to activate p53 reporter gene expression and to induce p53 (Cep-1)-mediated oocyte death (53–55).

We propose the balance in the relative activities of Ser/Thr phosphatase and ATM kinase during meiotic progression and oocyte development determines the final level of DNA DSB-induced TAp63α phosphorylation and, thereby, the level of death induced by either meiotic or IR-induced DNA DSBs (Fig. 7A). These mechanisms appear to be necessary to protect oocytes from meiotic DNA DSBs. Oocytes undergoing meiotic recombination may favor the balance in the two counteracting activities toward a higher phosphatase activity, whereas oocytes in dictyate arrest overcome phosphatase activity by TAp63α level-dependent transcriptional regulation of downstream target genes that may skew the balance toward a higher kinase activity (Fig. 7B). Further studies are required to test these possibilities.

Strategies that mimic DNA DSB formation and recovery in oocytes undergoing meiotic recombination may be the most effective approach to thwart radiation and chemotherapy-induced premature infertility in young women requiring cancer treatment (17, 58). Although blocking ATM activity (17) or the recently identified cell death-inducing downstream target genes of TAp63α, the PUMA and NOXA genes (15), are possible approaches, the downside of these strategies is that all of these factors are universally important in many cell types other than oocytes. On the other hand, TAp63α function is not universally required. Thus, the most target-specific approach may be to first identify the specific TAp63α phosphorylation sites that activate TAp63α death-inducing function. Approaches that directly target TAp63α activity may be a much more effective cell target-specific approach to sustaining female fertility after cancer treatment with few unwanted side effects.

ACKNOWLEDGMENTS

This research was supported by a Korean Research Foundation grant funded by the Korean government (MOEHRD), the Basic Science Research Promotion Fund (KRF-2008-531-C00044), and Basic Science Research Program/National Research Foundation of Korea grants (2009-0068266 and 2010-0025013) funded by the Ministry of Education, Science, and Technology.

REFERENCES

1. **Tilly JL.** 2001. Commuting the death sentence: how oocytes strive to survive. Nat. Rev. Mol. Cell. Biol. **2**:838–848. http://dx.doi.org/10.1038/35099086.

2. **Byskov AG.** 1986. Differentiation of mammalian embryonic gonad. Physiol. Rev. **66:**71–117.
3. **Di Giacomo M, Barchi M, Baudat F, Edelmann W, Keeney S, Jasin M.** 2005. Distinct DNA-damage-dependent and -independent responses drive the loss of oocytes in recombination-defective mouse mutants. Proc. Natl. Acad. Sci. U. S. A. **102:**737–742. http://dx.doi.org/10.1073/pnas.0406212102.
4. **Hanoux V, Pairault C, Bakalska M, Habert R, Livera G.** 2006. Caspase-2 involvement during ionizing radiation-induced oocyte death in the mouse ovary. Cell Death Differ. **14:**671–681. http://dx.doi.org/10.1038/sj.cdd.4402052.
5. **Rodrigues P, Limback D, McGinnis LK, Plancha CE, Albertini DF.** 2008. Oogenesis: prospects and challenges for the future. J. Cell Physiol. **216:**355–365. http://dx.doi.org/10.1002/jcp.21473.
6. **Morita Y, Tilly JL.** 1999. Oocyte apoptosis: like sand through an hourglass. Dev. Biol. **213:**1–17. http://dx.doi.org/10.1006/dbio.1999.9344.
7. **Yang A, Kaghad M, Wang Y, Gillett E, Fleming MD, Dötsch V, Andrews NC, Caput D, McKeon F.** 1998. p63, a p53 homolog at 3q27-29, encodes multiple products with transactivating, death-inducing, and dominant-negative activities. Mol. Cell **2:**305–316. http://dx.doi.org/10.1016/S1097-2765(00)80275-0.
8. **Müller M, Schleithoff ES, Stremmel W, Melino G, Krammer PH, Schilling T.** 2006. One, two, three: p53, p63, p73 and chemosensitivity. Drug Resist. Updates **9:**288–306. http://dx.doi.org/10.1016/j.drup.2007.01.001.
9. **Belyi VA, Ak P, Markert E, Wang H, Hu W, Puzio-Kuter A, Levine AJ.** 2010. The origins and evolution of the p53 family of genes. Cold Spring Harbor Perspect. Biol. **2:**a001198. http://dx.doi.org/10.1101/cshperspect.a001198.
10. **Crum CP, McKeon FD.** 2010. p63 in epithelial survival, germ cell surveillance, and neoplasia. Annu. Rev. Pathol. **5:**349–371. http://dx.doi.org/10.1146/annurev-pathol-121808-102117.
11. **Suh EK, Yang A, Kettenbach A, Bamberger C, Michaelis AH, Zhu Z, Elvin JA, Bronson RT, Crum CP, McKeon F.** 2006. p63 protects the female germ line during meiotic arrest. Nature **444:**624–628. http://dx.doi.org/10.1038/nature05337.
12. **Levine AJ, Tomasini R, McKeon FD, Mak TW, Melino G.** 2011. The p53 family: guardians of maternal reproduction. Nat. Rev. Mol. Cell. Biol. **12:**259–265. http://dx.doi.org/10.1038/nrm3086.
13. **Amelio I, Grespi F, Annicchiarico-Petruzzelli M, Melino G.** 2012. p63 the guardian of human reproduction. Cell Cycle **11:**4545–4551. http://dx.doi.org/10.4161/cc.22819.
14. **Deutsch GB, Zielonka EM, Coutandin D, Weber TA, Schäfer B, Hannewald J, Luh LM, Durst FG, Ibrahim M, Hoffmann J, Niesen FH, Senturk A, Kunkel H, Brutschy B, Schleiff E, Knapp S, Acker-Palmer A, Grez M, McKeon F, Dotsch V.** 2011. DNA damage in oocytes induces a switch of the quality control factor TAp63α from dimer to tetramer. Cell **144:**566–576. http://dx.doi.org/10.1016/j.cell.2011.01.013.
15. **Kerr JB, Hutt KJ, Michalak EM, Cook M, Vandenberg CJ, Liew SH, Bouillet P, Mills A, Scott CL, Findlay JK, Strasser A.** 2012. DNA damage-induced primordial follicle oocyte apoptosis and loss of fertility require TAp63-mediated induction of Puma and Noxa. Mol. Cell **48:**343–352. http://dx.doi.org/10.1016/j.molcel.2012.08.017.
16. **Livera G, Petre-Lazar B, Guerquin MJ, Trautmann E, Coffigny H, Habert R.** 2008. p63 null mutation protects mouse oocytes from radio-induced apoptosis. Reproduction **135:**3–12. http://dx.doi.org/10.1530/REP-07-0054.
17. **Gonfloni S, Di Tella L, Caldarola S, Cannata SM, Klinger FG, Di Bartolomeo C, Mattei M, Candi E, De Felici M, Melino G, Cesareni G.** 2009. Inhibition of the c-Abl-TAp63 pathway protects mouse oocytes from chemotherapy-induced death. Nat. Med. **15:**1179–1185. http://dx.doi.org/10.1038/nm.2033.
18. **Tilly JL, Niikura Y, Rueda BR.** 2009. The current status of evidence for and against postnatal oogenesis in mammals: a case of ovarian optimism versus pessimism? Biol. Reprod. **80:**2–12. http://dx.doi.org/10.1095/biolreprod.108.069088.
19. **Kerr JB, Hutt KJ, Cook M, Speed TP, Strasser A, Findlay JK, Scott CL.** 2012. Cisplatin-induced primordial follicle oocyte killing and loss of fertility are not prevented by imatinib. Nat. Med. **18:**1170–1172. http://dx.doi.org/10.1038/nm.2889.
20. **Maiani E, Di Bartolomeo C, Klinger FG, Cannata SM, Bernardini S, Chateauvieux S, Mack F, Mattei M, De Felici M, Diederich M, Cesareni G, Gonfloni S.** 2012. Reply to: Cisplatin-induced primordial follicle oocyte killing and loss of fertility are not prevented by imatinib. Nat. Med. **18:**1172–1174. http://dx.doi.org/10.1038/nm.2852.
21. **Keeney S, Baudat F, Angeles M, Zhou ZH, Copeland NG, Jenkins NA, Manova K, Jasin M.** 1999. A mouse homolog of the *Saccharomyces cerevisiae* meiotic recombination DNA transesterase Spo11p. Genomics **61:**170–182. http://dx.doi.org/10.1006/geno.1999.5956.
22. **Cohen PE, Pollack SE, Pollard JW.** 2006. Genetic analysis of chromosome pairing, recombination, and cell cycle control during first meiotic prophase in mammals. Endocrinol. Rev. **27:**398–426. http://dx.doi.org/10.1210/er.2005-0017.
23. **Hogan B, Beddington R, Costantini F, Lacey E.** 1994. Manipulating the mouse embryo: a laboratory manual, 2nd ed. Cold Spring Harbor Laboratory Press, New York, NY.
24. **Gosden R, Lee B.** 2010. Portrait of an oocyte: our obscure origin. J. Clin. Invest. **120:**973–983. http://dx.doi.org/10.1172/JCI41294.
25. **Racki WJ, Richter JD.** 2006. CPEB controls oocyte growth and follicle development in the mouse. Development **133:**4527–4537. http://dx.doi.org/10.1242/dev.02651.
26. **Ciccia A, Elledge SJ.** 2010. The DNA damage response: making it safe to play with knives. Mol. Cell **40:**179–204. http://dx.doi.org/10.1016/j.molcel.2010.09.019.
27. **Baudat F, Manova K, Yuen JP, Jasin M, Keeney S.** 2000. Chromosome synapsis defects and sexually dimorphic meiotic progression in mice lacking Spo11. Mol. Cell **6:**989–998. http://dx.doi.org/10.1016/S1097-2765(00)00098-8.
28. **Romanienko PJ, Camerini-Otero RD.** 2000. The mouse Spo11 gene is required for meiotic chromosome synapsis. Mol. Cell **5:**975–987.
29. **Lydall D, Nikolsky Y, Bishop DK, Weinert T.** 1996. A meiotic recombination checkpoint controlled by mitotic checkpoint genes. Nature **383:**840–843. http://dx.doi.org/10.1038/383840a0.
30. **Roeder GS, Bailis JM.** 2000. The pachytene checkpoint. Trends Genet. **16:**395–403. http://dx.doi.org/10.1016/S0168-9525(00)02080-1.
31. **Marcon E, Moens PB.** 2005. The evolution of meiosis: recruitment and modification of somatic DNA-repair proteins. Bioessays **27:**795–808. http://dx.doi.org/10.1002/bies.20264.
32. **Svetlanov A, Cohen PE.** 2004. Mismatch repair proteins, meiosis, and mice: understanding the complexities of mammalian meiosis. Exp. Cell Res. **296:**71–79. http://dx.doi.org/10.1016/j.yexcr.2004.03.020.
33. **Hunt PA, Hassold TJ.** 2002. Sex matters in meiosis. Science **296:**2181–2183. http://dx.doi.org/10.1126/science.1071907.
34. **Mostoslavsky G, Kotton DN, Fabian AJ, Gray JT, Lee JS, Mulligan RC.** 2005. Efficiency of transduction of highly purified murine hematopoietic stem cells by lentiviral and oncoretroviral vectors under conditions of minimal in vitro manipulation. Mol. Ther. **11:**932–940. http://dx.doi.org/10.1016/j.ymthe.2005.01.005.
35. **Banin S, Moyal L, Shieh S, Taya Y, Anderson CW, Chessa L, Smorodinsky NI, Prives C, Reiss Y, Shiloh Y, Ziv Y.** 1998. Enhanced phosphorylation of p53 by ATM in response to DNA damage. Science **281:**1674–1677. http://dx.doi.org/10.1126/science.281.5383.1674.
36. **Canman CE, Lim DS, Cimprich KA, Taya Y, Tamai K, Sakaguchi K, Appella E, Kastan MB, Siliciano JD.** 1998. Activation of the ATM kinase by ionizing radiation and phosphorylation of p53. Science **281:**1677–1679. http://dx.doi.org/10.1126/science.281.5383.1677.
37. **Burma S, Chen BP, Murphy M, Kurimasa A, Chen DJ.** 2001. ATM phosphorylates histone H2AX in response to DNA double-strand breaks. J. Biol. Chem. **276:**42462–42467. http://dx.doi.org/10.1074/jbc.C100466200.
38. **Bensimon A, Aebersold R, Shiloh Y.** 2011. Beyond ATM: the protein kinase landscape of the DNA damage response. FEBS Lett. **585:**1625–1639. http://dx.doi.org/10.1016/j.febslet.2011.05.013.
39. **Kim DA, Lee BL, Suh EK.** 2011. Ionizing radiation-induced TAp63alpha phosphorylation at C-terminal S/TQ motifs requires the N-terminal transactivation (TA) domain. Cell Cycle **10:**840–849. http://dx.doi.org/10.4161/cc.10.5.15008.
40. **Wymann MP, Bulgarelli-Leva G, Zvelebil MJ, Pirola L, Vanhaesebroeck B, Waterfield MD, Panayotou G.** 1996. Wortmannin inactivates phosphoinositide 3-kinase by covalent modification of Lys-802, a residue involved in the phosphate transfer reaction. Mol. Cell. Biol. **4:**1722–1733.
41. **Bakkenist CJ, Kastan MB.** 2003. DNA damage activates ATM through intermolecular autophosphorylation and dimer dissociation. Nature **421:**499–506. http://dx.doi.org/10.1038/nature01368.
42. **Paull TT, Rogakou EP, Yamazaki V, Kirchgessner CU, Gellert M, Bonner WM.** 2000. A critical role for histone H2AX in recruitment of

repair factors to nuclear foci after DNA damage. Curr. Biol. **10:**886–895. http://dx.doi.org/10.1016/S0960-9822(00)00610-2.
43. **Peng A, Maller JL.** 2010. Serine/threonine phosphatases in the DNA damage response and cancer. Oncogene **29:**5977–5988. http://dx.doi.org/10.1038/onc.2010.371.
44. **Peng A, Lewellyn AL, Schiemann WP, Maller JL.** 2010. Repo-man controls a protein phosphatase 1-dependent threshold for DNA damage checkpoint activation. Curr. Biol. **20:**387–396. http://dx.doi.org/10.1016/j.cub.2010.01.020.
45. **Marangos P, Carroll J.** 2012. Oocytes progress beyond prophase in the presence of DNA damage. Curr. Biol. **22:**989–994. http://dx.doi.org/10.1016/j.cub.2012.03.063.
46. **Turner JM, Mahadevaiah SK, Fernandez-Capetillo O, Nussenzweig A, Xu X, Deng CX, Burgoyne PS.** 2005. Silencing of unsynapsed meiotic chromosomes in the mouse. Nat. Genet. **1:**41–47. http://dx.doi.org/10.1038/ng1484.
47. **Shafman T, Khanna KK, Kedar P, Spring K, Kozlov S, Yen T, Hobson K, Gatei M, Zhang N, Watters D, Egerton M, Shiloh Y, Kharbanda S, Kufe D, Lavin MF.** 1997. Interaction between ATM protein and c-Abl in response to DNA damage. Nature **387:**520–523. http://dx.doi.org/10.1038/387520a0.
48. **Wang X, Zeng L, Wang J, Chau JF, Lai KP, Jia D, Poonepalli A, Hande MP, Liu H, He G, He L, Li B.** 2011. A positive role for c-Abl in Atm and Atr activation in DNA damage response. Cell Death Differ. **18:**5–15. http://dx.doi.org/10.1038/cdd.2010.106.
49. **Deng X, Hofmann ER, Villanueva A, Hobert O, Capodieci P, Veach DR, Yin X, Campodonico L, Glekas A, Cordon-Cardo C, Clarkson B, Bornmann WG, Fuks Z, Hengartner MO, Kolesnick R.** 2004. *Caenorhabditis elegans* ABL-1 antagonizes p53-mediated germline apoptosis after ionizing irradiation. Nat. Genet. **36:**906–912. http://dx.doi.org/10.1038/ng1396.
50. **Rutkowski R, Dickinson R, Stewart G, Craig A, Schimpl M, Keyse SM, Gartner A.** 2011. Regulation of *Caenorhabditis elegans* p53/CEP-1-dependent germ cell apoptosis by Ras/MAPK signaling. PLoS Genet. **8:**e1002238. http://dx.doi.org/10.1371/journal.pgen.1002238.
51. **Tomasini R, Tsuchihara K, Wilhelm M, Fujitani M, Rufini A, Cheung CC, Khan F, Itie-Youten A, Wakeham A, Tsao MS, Iovanna JL, Squire J, Jurisica I, Kaplan D, Melino G, Jurisicova A, Mak TW.** 2008. TAp73 knockout shows genomic instability with infertility and tumor suppressor functions. Genes Dev. **22:**2677–2691. http://dx.doi.org/10.1101/gad.1695308.
52. **Tomasini R, Tsuchihara K, Tsuda C, Lau SK, Wilhelm M, Ruffini A, Tsao MS, Iovanna JL, Jurisicova A, Melino G, Mak TW.** 2009. TAp73 regulates the spindle assembly checkpoint by modulating BubR1 activity. Proc. Natl. Acad. Sci. U. S. A. **106:**797–802. http://dx.doi.org/10.1073/pnas.0812096106.
53. **Lu WJ, Chapo J, Roig I, Abrams JM.** 2010. Meiotic recombination provokes functional activation of the p53 regulatory network. Science **328:**1278–1281. http://dx.doi.org/10.1126/science.1185640.
54. **Derry WB, Putzke AP, Rothman JH.** 2001. *Caenorhabditis elegans* p53: role in apoptosis, meiosis, and stress resistance. Science **294:**591–595. http://dx.doi.org/10.1126/science.1065486.
55. **Schumacher B, Hofmann K, Boulton S, Gartner A.** 2001. The *Caenorhabditis elegans* homolog of the p53 tumor suppressor is required for DNA damage-induced apoptosis. Curr. Biol. **11:**1722–1727. http://dx.doi.org/10.1016/S0960-9822(01)00534-6.
56. **Al Rashid ST, Dellaire G, Cuddihy A, Jalai F, Vaid M, Coackly C, Folkard M, Xu Y, Chen DJ, Lilge L, Prise KM, Bazett Jones DP, Bristow RG.** 2005. Evidence for the direct binding of phosphorylated p53 to sites of DNA breaks in vivo. Cancer Res. **65:**10810–10821. http://dx.doi.org/10.1158/0008-5472.CAN-05-0729.
57. **Wittlinger M, Grabenbauer GG, Sprung CN, Sauer R, Distel LV.** 2007. Time- and dose-dependent activation of p53 serine 15 phosphorylation among cell lines with different radiation sensitivity. Int. J. Radiat. Biol. **83:**245–257. http://dx.doi.org/10.1080/09553000701275432.
58. **Perez GI, Knudson CM, Leykin L, Korsmeyer SJ, Tilly JL.** 1997. Apoptosis-associated signaling pathways are required for chemotherapy-mediated female germ cell destruction. Nat. Med. **3:**1228–1232. http://dx.doi.org/10.1038/nm1197-1228.